Supplementary Materials for “IMIX: A multivariate mixture model approach to association analysis through multi-omics data integration”

Ziqiao Wang[1,2] and Peng Wei[1,*]

[1]Department of Biostatistics, The University of Texas MD Anderson Cancer Center, Houston, Texas, USA
[2]The University of Texas MD Anderson Cancer Center UTHealth Graduate School of Biomedical Sciences, Houston, Texas, USA

1 Details on the EM algorithm

1.1 IMIX-Ind

To infer whether gene i is associated with data type h, we use the posterior probability

$$\begin{aligned} Pr(z_{ik}=1|X_{i1},X_{i2},X_{i3},\boldsymbol{\theta}) =& \frac{\pi_k f_k(X_{i1},X_{i2},X_{i3})}{\sum_{j=1}^{K}\pi_j f_j(X_{i1},X_{i2},X_{i3})} \\ =& \frac{\pi_k f_{k1}(X_{i1};\theta_{k1}) f_{k2}(X_{i2};\theta_{k2}) f_{k3}(X_{i3};\theta_{k3})}{f(X_{i1},X_{i2},X_{i3})}. \end{aligned}$$

Notice that here we assume $K=8$. For each scenario, it corresponds as:

K=1: (0,0,0); K=2: (1,0,0); K=3: (0,1,0); K=4: (0,0,1); K=5: (1,1,0); K=6: (1,0,1); K=7: (0,1,1); K=8: (1,1,1).

[*]Correspondence should be addressed to: Peng Wei, PhD, 1400 Pressler St, Unit 1411, Department of Biostatistics, The University of Texas MD Anderson Cancer Center, Houston, TX 77030, USA; Email: pwei2@mdanderson.org

We assume $f_{kh} = \phi(.;\mu_{kh},\sigma_{kh})$, a normal probability density function with mean μ_{kh} and variance σ_{kh}^2, $k = 1,\cdots,8; h = 1,2,3$. Thus we have

$$\begin{aligned}
f(X_{i1},X_{i2},X_{i3}) =& \sum_{k=1}^{K} \pi_k f_k(x_1,x_2,x_3) \\
=& \sum_{k=1}^{K} \pi_k f_{k1}(x_1;\theta_{k1}) f_{k2}(x_2;\theta_{k2}) f_{k3}(x_3;\theta_{k3}) \\
=& \pi_1 f(x_1;\mu_{10},\sigma_{10}) f(x_2;\mu_{20},\sigma_{20}) f(x_3;\mu_{30},\sigma_{30}) \\
+& \pi_2 f(x_1;\mu_{11},\sigma_{11}) f(x_2;\mu_{20},\sigma_{20}) f(x_3;\mu_{30},\sigma_{30}) \\
+& \pi_3 f(x_1;\mu_{10},\sigma_{10}) f(x_2;\mu_{21},\sigma_{21}) f(x_3;\mu_{30},\sigma_{30}) \\
+& \pi_4 f(x_1;\mu_{10},\sigma_{10}) f(x_2;\mu_{20},\sigma_{20}) f(x_3;\mu_{31},\sigma_{31}) \\
+& \pi_5 f(x_1;\mu_{11},\sigma_{11}) f(x_2;\mu_{21},\sigma_{21}) f(x_3;\mu_{30},\sigma_{30}) \\
+& \pi_6 f(x_1;\mu_{11},\sigma_{11}) f(x_2;\mu_{20},\sigma_{20}) f(x_3;\mu_{31},\sigma_{31}) \\
+& \pi_7 f(x_1;\mu_{10},\sigma_{10}) f(x_2;\mu_{21},\sigma_{21}) f(x_3;\mu_{31},\sigma_{31}) \\
+& \pi_8 f(x_1;\mu_{11},\sigma_{11}) f(x_2;\mu_{21},\sigma_{21}) f(x_3;\mu_{31},\sigma_{31}).
\end{aligned}$$

$$\begin{aligned}
&\mu_{11} = \mu_{31} = \mu_{41} = \mu_{71} \overset{\triangle}{=} \mu_{10}, \sigma_{11} = \sigma_{31} = \sigma_{41} = \sigma_{71} \overset{\triangle}{=} \sigma_{10} \\
&\mu_{12} = \mu_{22} = \mu_{42} = \mu_{62} \overset{\triangle}{=} \mu_{20}, \sigma_{12} = \sigma_{22} = \sigma_{42} = \sigma_{62} \overset{\triangle}{=} \sigma_{20} \\
&\mu_{13} = \mu_{23} = \mu_{33} = \mu_{53} \overset{\triangle}{=} \mu_{30}, \sigma_{13} = \sigma_{23} = \sigma_{33} = \sigma_{43} \overset{\triangle}{=} \sigma_{30} \\
&\mu_{21} = \mu_{51} = \mu_{61} = \mu_{81} \overset{\triangle}{=} \mu_{11}, \sigma_{21} = \sigma_{51} = \sigma_{61} = \sigma_{81} \overset{\triangle}{=} \sigma_{11} \\
&\mu_{32} = \mu_{52} = \mu_{72} = \mu_{82} \overset{\triangle}{=} \mu_{21}, \sigma_{32} = \sigma_{52} = \sigma_{72} = \sigma_{82} \overset{\triangle}{=} \sigma_{21} \\
&\mu_{43} = \mu_{63} = \mu_{73} = \mu_{83} \overset{\triangle}{=} \mu_{31}, \sigma_{43} = \sigma_{63} = \sigma_{73} = \sigma_{83} \overset{\triangle}{=} \sigma_{31}.
\end{aligned}$$

For the EM algorithm, the complete log-likelihood is

$$\log L_c = \sum_{i=1}^{N}\sum_{k=1}^{K} z_{ik} \log \pi_k f_k(X_{i1}, X_{i2}, X_{i3}).$$

The E-step is to calculate the conditional expectation

$$Q = E(\log L_c | data) = \sum_{i=1}^{N}\sum_{k=1}^{K} \tau(z_{ik}) \log \pi_k f_k(X_{i1}, X_{i2}, X_{i3}),$$

where $\tau(z_{ik}) = Pr(z_{ik} = 1 | X_{i1}, X_{i2}, X_{i3})$. The M-step maximized the above Q with respect to the unknown parameters:

E step: Compute $\tau(z_{ik})$ with current parameter $\boldsymbol{\theta}^{(m)} = \{\pi_k^{(m)}, \mu_{kh}^{(m)}, \sigma_{kh}^{2\ (m)}\}$ at each iteration m:

$$\tau(z_{ik}) = Pr(z_{ik} = 1 | X_{i1}, X_{i2}, X_{i3}) = \frac{\pi_k^{(m)} f_k^{(m)}(X_{i1}, X_{i2}, X_{i3})}{\sum_{j=1}^{K} \pi_j^{(m)} f_j^{(m)}(X_{i1}, X_{i2}, X_{i3})},$$

where $f_k^{(m)}(X_{i1}, X_{i2}, X_{i3}) = \prod_{h=1}^{3} \phi(X_{ih}; \mu_{kh}^{(m)}, \sigma_{kh}^{(m)})$.

M step: Update $\boldsymbol{\theta}^{(m)}$ and replace by $\boldsymbol{\theta}^{(m+1)}$:

$$
\begin{aligned}
\pi_k^{(m+1)} =& \frac{\sum_{i=1}^N \tau(z_{ik})}{N}, \\
\mu_{10}^{(m+1)} =& \frac{\sum_{i=1}^N X_{i1}(\tau(z_{i1}) + \tau(z_{i3}) + \tau(z_{i4}) + \tau(z_{i7}))}{\sum_{i=1}^N (\tau(z_{i1}) + \tau(z_{i3}) + \tau(z_{i4}) + \tau(z_{i7}))}, \\
\mu_{20}^{(m+1)} =& \frac{\sum_{i=1}^N X_{i2}(\tau(z_{i1}) + \tau(z_{i2}) + \tau(z_{i4}) + \tau(z_{i6}))}{\sum_{i=1}^N (\tau(z_{i1}) + \tau(z_{i2}) + \tau(z_{i4}) + \tau(z_{i6}))}, \\
\mu_{30}^{(m+1)} =& \frac{\sum_{i=1}^N X_{i3}(\tau(z_{i1}) + \tau(z_{i2}) + \tau(z_{i3}) + \tau(z_{i5}))}{\sum_{i=1}^N (\tau(z_{i1}) + \tau(z_{i2}) + \tau(z_{i3}) + \tau(z_{i5}))}, \\
\mu_{11}^{(m+1)} =& \frac{\sum_{i=1}^N X_{i1}(\tau(z_{i2}) + \tau(z_{i5}) + \tau(z_{i6}) + \tau(z_{i8}))}{\sum_{i=1}^N (\tau(z_{i2}) + \tau(z_{i5}) + \tau(z_{i6}) + \tau(z_{i8}))}, \\
\mu_{21}^{(m+1)} =& \frac{\sum_{i=1}^N X_{i2}(\tau(z_{i3}) + \tau(z_{i5}) + \tau(z_{i7}) + \tau(z_{i8}))}{\sum_{i=1}^N (\tau(z_{i3}) + \tau(z_{i5}) + \tau(z_{i7}) + \tau(z_{i8}))}, \\
\mu_{31}^{(m+1)} =& \frac{\sum_{i=1}^N X_{i3}(\tau(z_{i4}) + \tau(z_{i6}) + \tau(z_{i7}) + \tau(z_{i8}))}{\sum_{i=1}^N (\tau(z_{i4}) + \tau(z_{i6}) + \tau(z_{i7}) + \tau(z_{i8}))}, \\
{\sigma_{10}^2}^{(m+1)} =& \frac{\sum_{i=1}^N (X_{i1} - \mu_{10}^{(m+1)})^2(\tau(z_{i1}) + \tau(z_{i3}) + \tau(z_{i4}) + \tau(z_{i7}))}{\sum_{i=1}^N (\tau(z_{i1}) + \tau(z_{i3}) + \tau(z_{i4}) + \tau(z_{i7}))}, \\
{\sigma_{20}^2}^{(m+1)} =& \frac{\sum_{i=1}^N (X_{i2} - \mu_{20}^{(m+1)})^2(\tau(z_{i1}) + \tau(z_{i2}) + \tau(z_{i4}) + \tau(z_{i6}))}{\sum_{i=1}^N (\tau(z_{i1}) + \tau(z_{i2}) + \tau(z_{i4}) + \tau(z_{i6}))}, \\
{\sigma_{30}^2}^{(m+1)} =& \frac{\sum_{i=1}^N (X_{i3} - \mu_{30}^{(m+1)})^2(\tau(z_{i1}) + \tau(z_{i2}) + \tau(z_{i3}) + \tau(z_{i5}))}{\sum_{i=1}^N (\tau(z_{i1}) + \tau(z_{i2}) + \tau(z_{i3}) + \tau(z_{i5}))}, \\
{\sigma_{11}^2}^{(m+1)} =& \frac{\sum_{i=1}^N (X_{i1} - \mu_{11}^{(m+1)})^2(\tau(z_{i2}) + \tau(z_{i5}) + \tau(z_{i6}) + \tau(z_{i8}))}{\sum_{i=1}^N (\tau(z_{i2}) + \tau(z_{i5}) + \tau(z_{i6}) + \tau(z_{i8}))}, \\
{\sigma_{21}^2}^{(m+1)} =& \frac{\sum_{i=1}^N (X_{i2} - \mu_{21}^{(m+1)})^2(\tau(z_{i3}) + \tau(z_{i5}) + \tau(z_{i7}) + \tau(z_{i8}))}{\sum_{i=1}^N (\tau(z_{i3}) + \tau(z_{i5}) + \tau(z_{i7}) + \tau(z_{i8}))}, \\
{\sigma_{31}^2}^{(m+1)} =& \frac{\sum_{i=1}^N (X_{i3} - \mu_{31}^{(m+1)})^2(\tau(z_{i4}) + \tau(z_{i6}) + \tau(z_{i7}) + \tau(z_{i8}))}{\sum_{i=1}^N (\tau(z_{i4}) + \tau(z_{i6}) + \tau(z_{i7}) + \tau(z_{i8}))}.
\end{aligned}
$$

Repeat the above iterations until convergence.

1.2 IMIX-Cor

We assume that the three data sources can be summarized as (X_{i1}, X_{i2}, X_{i3}) for each gene $i, i = 1, \cdots, N$, data type $h = 1, 2, 3$: $X_{ih} = \Phi^{-1}(p_{ih})$, p_{ih} is the p-values. We assume that (X_{i1}, X_{i2}, X_{i3}) comes from a mixture distribution with K mixture components:

$$f(x_1, x_2, x_3) = \sum_{k=1}^{K} \pi_k f_k(x_1, x_2, x_3).$$

To infer whether gene i is associated with data type h, we use the posterior probability

$$Pr(z_{ik} = 1 | X_{i1}, X_{i2}, X_{i3}, \boldsymbol{\theta}) = \frac{\pi_k f_k(X_{i1}, X_{i2}, X_{i3})}{\sum_{j=1}^{K} \pi_j f_j(X_{i1}, X_{i2}, X_{i3})}.$$

Notice that here we assume $K = 8$. For each scenario, it corresponds as:
K=1: (0,0,0); K=2: (1,0,0); K=3: (0,1,0); K=4: (0,0,1); K=5: (1,1,0); K=6: (1,0,1); K=7: (0,1,1); K=8: (1,1,1).

We assume $f_k = N(\boldsymbol{\mu_k, \Sigma_k})$ with mixing proportion $\pi_k, k = 1, \cdots, 8$. Here we add a constrain on the $\boldsymbol{\mu}_k$:

$$\boldsymbol{\mu_1} = (\mu_{10}, \mu_{20}, \mu_{30}); \boldsymbol{\mu_2} = (\mu_{11}, \mu_{20}, \mu_{30});$$

$$\boldsymbol{\mu_3} = (\mu_{10}, \mu_{21}, \mu_{30}); \boldsymbol{\mu_4} = (\mu_{10}, \mu_{20}, \mu_{31});$$

$$\boldsymbol{\mu_5} = (\mu_{11}, \mu_{21}, \mu_{30}); \boldsymbol{\mu_6} = (\mu_{11}, \mu_{20}, \mu_{31});$$

$$\boldsymbol{\mu_7} = (\mu_{10}, \mu_{21}, \mu_{31}); \boldsymbol{\mu_8} = (\mu_{11}, \mu_{21}, \mu_{31}).$$

The complete log-likelihood is

$$\log L_c = \sum_{i=1}^{N}\sum_{k=1}^{K} z_{ik} \log \pi_k f_k(X_{i1}, X_{i2}, X_{i3}).$$

The E-step is to calculate the conditional expectation

$$Q = E(\log L_c|data) = \sum_{i=1}^{N}\sum_{k=1}^{K} \tau(z_{ik}) \log \pi_k f_k(X_{i1}, X_{i2}, X_{i3}).$$

where $\tau(z_{ik}) = Pr(z_{ik} = 1|X_{i1}, X_{i2}, X_{i3})$. The M-step maximized the above Q with respect to the unknown parameters, for the unconstrained model:

E step: Compute $\tau(z_{ik})$ with current parameter $\boldsymbol{\theta}^{(m)} = \{\pi_k^{(m)}, \boldsymbol{\mu_k}^{(m)}, \boldsymbol{\Sigma_k}^{(m)}\}$ at each iteration m:

$$\tau(z_{ik}) = Pr(z_{ik} = 1|X_{i1}, X_{i2}, X_{i3}) = \frac{\pi_k^{(m)} f_k^{(m)}(X_{i1}, X_{i2}, X_{i3})}{\sum_{j=1}^{K} \pi_j^{(m)} f_j^{(m)}(X_{i1}, X_{i2}, X_{i3})},$$

where $f_k^{(m)}(X_{i1}, X_{i2}, X_{i3}) = \mathcal{N}(\boldsymbol{X_i}|\boldsymbol{\mu_k}^{(m)}, \boldsymbol{\Sigma_k}^{(m)})$.

M step: Update $\boldsymbol{\theta}^{(m)}$ and replace by $\boldsymbol{\theta}^{(m+1)}$:

$$\begin{aligned}
\pi_k^{(m+1)} &= \frac{\sum_{i=1}^{N} \tau(z_{ik})}{N}, \\
\boldsymbol{\mu}_k^{(m+1)} &= \frac{\sum_{i=1}^{N} \tau(z_{ik}) \boldsymbol{X_i}}{\sum_{i=1}^{N} \tau(z_{ik})}, \\
\Sigma_k{}^{(m+1)} &= \frac{\sum_{i=1}^{N} \tau(z_{ik})(\boldsymbol{X_i} - \boldsymbol{\mu}_k^{(m+1)})^T(\boldsymbol{X_i} - \boldsymbol{\mu}_k^{(m+1)})}{\sum_{i=1}^{N} \tau(z_{ik})}.
\end{aligned}$$

Repeat the above iterations until convergence.

1.3 IMIX-Cor-Restrict

We conduct the EM algorithm similarly to IMIX-Cor with an restriction imposed on $\boldsymbol{\mu_k}$, we define

$$\boldsymbol{\Sigma_k^{-1}} = \begin{pmatrix} a_{11}^{(k)} & a_{12}^{(k)} & a_{13}^{(k)} \\ a_{12}^{(k)} & a_{22}^{(k)} & a_{23}^{(k)} \\ a_{13}^{(k)} & a_{23}^{(k)} & a_{33}^{(k)} \end{pmatrix}, \quad k = 1, \cdots, 8.$$

then $\boldsymbol{\mu}_k$ can be updated as:

$$
\begin{aligned}
\mu_{10}^{(m+1)} =& \frac{\sum_{i=1}^{N} X_{i1}\left(a_{11}^{(1)}\tau(z_{i1}) + a_{11}^{(3)}\tau(z_{i3}) + a_{11}^{(4)}\tau(z_{i4}) + a_{11}^{(7)}\tau(z_{i7})\right)}{\sum_{i=1}^{N}\left(a_{11}^{(1)}\tau(z_{i1}) + a_{11}^{(3)}\tau(z_{i3}) + a_{11}^{(4)}\tau(z_{i4}) + a_{11}^{(7)}\tau(z_{i7})\right)} \\
&+ \frac{\sum_{i=1}^{N}\left((X_{i2} - \mu_{20}^{(m)})(a_{12}^{(1)}\tau(z_{i1}) + a_{12}^{(4)}\tau(z_{i4})) + (X_{i2} - \mu_{21}^{(m)})(a_{12}^{(3)}\tau(z_{i3}) + a_{12}^{(7)}\tau(z_{i7}))\right)}{\sum_{i=1}^{N}\left(a_{11}^{(1)}\tau(z_{i1}) + a_{11}^{(3)}\tau(z_{i3}) + a_{11}^{(4)}\tau(z_{i4}) + a_{11}^{(7)}\tau(z_{i7})\right)} \\
&+ \frac{\sum_{i=1}^{N}\left((X_{i3} - \mu_{30}^{(m)})(a_{13}^{(1)}\tau(z_{i1}) + a_{13}^{(3)}\tau(z_{i3})) + (X_{i3} - \mu_{31}^{(m)})(a_{13}^{(4)}\tau(z_{i4}) + a_{13}^{(7)}\tau(z_{i7}))\right)}{\sum_{i=1}^{N}\left(a_{11}^{(1)}\tau(z_{i1}) + a_{11}^{(3)}\tau(z_{i3}) + a_{11}^{(4)}\tau(z_{i4}) + a_{11}^{(7)}\tau(z_{i7})\right)}, \\
\mu_{20}^{(m+1)} =& \frac{\sum_{i=1}^{N} X_{i2}\left(a_{22}^{(1)}\tau(z_{i1}) + a_{22}^{(2)}\tau(z_{i2}) + a_{22}^{(4)}\tau(z_{i4}) + a_{22}^{(6)}\tau(z_{i6})\right)}{\sum_{i=1}^{N}\left(a_{22}^{(1)}\tau(z_{i1}) + a_{22}^{(2)}\tau(z_{i2}) + a_{22}^{(4)}\tau(z_{i4}) + a_{22}^{(6)}\tau(z_{i6})\right)} \\
&+ \frac{\sum_{i=1}^{N}\left((X_{i1} - \mu_{10}^{(m)})(a_{12}^{(1)}\tau(z_{i1}) + a_{12}^{(4)}\tau(z_{i4})) + (X_{i1} - \mu_{11}^{(m)})(a_{12}^{(2)}\tau(z_{i2}) + a_{12}^{(6)}\tau(z_{i6}))\right)}{\sum_{i=1}^{N}\left(a_{22}^{(1)}\tau(z_{i1}) + a_{22}^{(2)}\tau(z_{i2}) + a_{22}^{(4)}\tau(z_{i4}) + a_{22}^{(6)}\tau(z_{i6})\right)} \\
&+ \frac{\sum_{i=1}^{N}\left((X_{i3} - \mu_{30}^{(m)})(a_{23}^{(1)}\tau(z_{i1}) + a_{23}^{(2)}\tau(z_{i2})) + (X_{i3} - \mu_{31}^{(m)})(a_{23}^{(4)}\tau(z_{i4}) + a_{23}^{(6)}\tau(z_{i6}))\right)}{\sum_{i=1}^{N}\left(a_{22}^{(1)}\tau(z_{i1}) + a_{22}^{(2)}\tau(z_{i2}) + a_{22}^{(4)}\tau(z_{i4}) + a_{22}^{(6)}\tau(z_{i6})\right)}, \\
\mu_{30}^{(m+1)} =& \frac{\sum_{i=1}^{N} X_{i3}\left(a_{33}^{(1)}\tau(z_{i1}) + a_{33}^{(2)}\tau(z_{i2}) + a_{33}^{(3)}\tau(z_{i3}) + a_{33}^{(5)}\tau(z_{i5})\right)}{\sum_{i=1}^{N}\left(a_{33}^{(1)}\tau(z_{i1}) + a_{33}^{(2)}\tau(z_{i2}) + a_{33}^{(3)}\tau(z_{i3}) + a_{33}^{(5)}\tau(z_{i5})\right)} \\
&+ \frac{\sum_{i=1}^{N}\left((X_{i1} - \mu_{10}^{(m)})(a_{13}^{(1)}\tau(z_{i1}) + a_{13}^{(3)}\tau(z_{i3})) + (X_{i1} - \mu_{11}^{(m)})(a_{13}^{(2)}\tau(z_{i2}) + a_{13}^{(5)}\tau(z_{i5}))\right)}{\sum_{i=1}^{N}\left(a_{33}^{(1)}\tau(z_{i1}) + a_{33}^{(2)}\tau(z_{i2}) + a_{33}^{(3)}\tau(z_{i3}) + a_{33}^{(5)}\tau(z_{i5})\right)} \\
&+ \frac{\sum_{i=1}^{N}\left((X_{i2} - \mu_{20}^{(m)})(a_{23}^{(1)}\tau(z_{i1}) + a_{23}^{(2)}\tau(z_{i2})) + (X_{i2} - \mu_{21}^{(m)})(a_{23}^{(3)}\tau(z_{i3}) + a_{23}^{(5)}\tau(z_{i5}))\right)}{\sum_{i=1}^{N}\left(a_{33}^{(1)}\tau(z_{i1}) + a_{33}^{(2)}\tau(z_{i2}) + a_{33}^{(3)}\tau(z_{i3}) + a_{33}^{(5)}\tau(z_{i5})\right)}, \\
\mu_{11}^{(m+1)} =& \frac{\sum_{i=1}^{N} X_{i1}\left(a_{11}^{(2)}\tau(z_{i2}) + a_{11}^{(5)}\tau(z_{i5}) + a_{11}^{(6)}\tau(z_{i6}) + a_{11}^{(8)}\tau(z_{i8})\right)}{\sum_{i=1}^{N}\left(a_{11}^{(2)}\tau(z_{i2}) + a_{11}^{(5)}\tau(z_{i5}) + a_{11}^{(6)}\tau(z_{i6}) + a_{11}^{(8)}\tau(z_{i8})\right)} \\
&+ \frac{\sum_{i=1}^{N}\left((X_{i2} - \mu_{20}^{(m)})(a_{12}^{(2)}\tau(z_{i2}) + a_{12}^{(6)}\tau(z_{i6})) + (X_{i2} - \mu_{21}^{(m)})(a_{12}^{(5)}\tau(z_{i5}) + a_{12}^{(8)}\tau(z_{i8}))\right)}{\sum_{i=1}^{N}\left(a_{11}^{(2)}\tau(z_{i2}) + a_{11}^{(5)}\tau(z_{i5}) + a_{11}^{(6)}\tau(z_{i6}) + a_{11}^{(8)}\tau(z_{i8})\right)} \\
&+ \frac{\sum_{i=1}^{N}\left((X_{i3} - \mu_{30}^{(m)})(a_{13}^{(2)}\tau(z_{i2}) + a_{13}^{(5)}\tau(z_{i5})) + (X_{i3} - \mu_{31}^{(m)})(a_{13}^{(6)}\tau(z_{i6}) + a_{13}^{(8)}\tau(z_{i8}))\right)}{\sum_{i=1}^{N}\left(a_{11}^{(2)}\tau(z_{i2}) + a_{11}^{(5)}\tau(z_{i5}) + a_{11}^{(6)}\tau(z_{i6}) + a_{11}^{(8)}\tau(z_{i8})\right)}, \\
\mu_{21}^{(m+1)} =& \frac{\sum_{i=1}^{N} X_{i2}\left(a_{22}^{(3)}\tau(z_{i3}) + a_{22}^{(5)}\tau(z_{i5}) + a_{22}^{(7)}\tau(z_{i7}) + a_{22}^{(8)}\tau(z_{i8})\right)}{\sum_{i=1}^{N}\left(a_{22}^{(3)}\tau(z_{i3}) + a_{22}^{(5)}\tau(z_{i5}) + a_{22}^{(7)}\tau(z_{i7}) + a_{22}^{(8)}\tau(z_{i8})\right)} \\
&+ \frac{\sum_{i=1}^{N}\left((X_{i1} - \mu_{10}^{(m)})(a_{12}^{(3)}\tau(z_{i3}) + a_{12}^{(7)}\tau(z_{i7})) + (X_{i1} - \mu_{11}^{(m)})(a_{12}^{(5)}\tau(z_{i5}) + a_{12}^{(8)}\tau(z_{i8}))\right)}{\sum_{i=1}^{N}\left(a_{22}^{(3)}\tau(z_{i3}) + a_{22}^{(5)}\tau(z_{i5}) + a_{22}^{(7)}\tau(z_{i7}) + a_{22}^{(8)}\tau(z_{i8})\right)} \\
&+ \frac{\sum_{i=1}^{N}\left((X_{i3} - \mu_{30}^{(m)})(a_{23}^{(3)}\tau(z_{i3}) + a_{23}^{(5)}\tau(z_{i5})) + (X_{i3} - \mu_{31}^{(m)})(a_{23}^{(7)}\tau(z_{i7}) + a_{23}^{(8)}\tau(z_{i8}))\right)}{\sum_{i=1}^{N}\left(a_{22}^{(3)}\tau(z_{i3}) + a_{22}^{(5)}\tau(z_{i5}) + a_{22}^{(7)}\tau(z_{i7}) + a_{22}^{(8)}\tau(z_{i8})\right)}, \\
\mu_{31}^{(m+1)} =& \frac{\sum_{i=1}^{N} X_{i3}\left(a_{33}^{(4)}\tau(z_{i4}) + a_{33}^{(6)}\tau(z_{i6}) + a_{33}^{(7)}\tau(z_{i7}) + a_{33}^{(8)}\tau(z_{i8})\right)}{\sum_{i=1}^{N}\left(a_{33}^{(4)}\tau(z_{i4}) + a_{33}^{(6)}\tau(z_{i6}) + a_{33}^{(7)}\tau(z_{i7}) + a_{33}^{(8)}\tau(z_{i8})\right)} \\
&+ \frac{\sum_{i=1}^{N}\left((X_{i1} - \mu_{10}^{(m)})(a_{13}^{(4)}\tau(z_{i4}) + a_{13}^{(7)}\tau(z_{i7})) + (X_{i1} - \mu_{11}^{(m)})(a_{13}^{(6)}\tau(z_{i6}) + a_{13}^{(8)}\tau(z_{i8}))\right)}{\sum_{i=1}^{N}\left(a_{33}^{(4)}\tau(z_{i4}) + a_{33}^{(6)}\tau(z_{i6}) + a_{33}^{(7)}\tau(z_{i7}) + a_{33}^{(8)}\tau(z_{i8})\right)} \\
&+ \frac{\sum_{i=1}^{N}\left((X_{i2} - \mu_{20}^{(m)})(a_{23}^{(4)}\tau(z_{i4}) + a_{23}^{(6)}\tau(z_{i6})) + (X_{i2} - \mu_{21}^{(m)})(a_{23}^{(7)}\tau(z_{i7}) + a_{23}^{(8)}\tau(z_{i8}))\right)}{\sum_{i=1}^{N}\left(a_{33}^{(4)}\tau(z_{i4}) + a_{33}^{(6)}\tau(z_{i6}) + a_{33}^{(7)}\tau(z_{i7}) + a_{33}^{(8)}\tau(z_{i8})\right)}.
\end{aligned}
$$

For two data types, we define

$$\boldsymbol{\Sigma_k^{-1}} = \begin{pmatrix} a_{11}^{(k)} & a_{12}^{(k)} \\ a_{12}^{(k)} & a_{22}^{(k)} \end{pmatrix}, \quad k = 1, \cdots, 4$$

then $\boldsymbol{\mu}_k$ can be updated as:

$$\begin{aligned}
\mu_{10}^{(m+1)} =& \frac{\sum_{i=1}^N X_{i1}\left(a_{11}^{(1)}\tau(z_{i1}) + a_{11}^{(3)}\tau(z_{i3})\right)}{\sum_{i=1}^N \left(a_{11}^{(1)}\tau(z_{i1}) + a_{11}^{(3)}\tau(z_{i3})\right)} \\
&+ \frac{\sum_{i=1}^N \left((X_{i2} - \mu_{20}^{(m)})a_{12}^{(1)}\tau(z_{i1}) + (X_{i2} - \mu_{21}^{(m)})a_{12}^{(3)}\tau(z_{i3})\right)}{\sum_{i=1}^N \left(a_{11}^{(1)}\tau(z_{i1}) + a_{11}^{(3)}\tau(z_{i3})\right)} \\
\mu_{20}^{(m+1)} =& \frac{\sum_{i=1}^N X_{i2}\left(a_{22}^{(1)}\tau(z_{i1}) + a_{22}^{(2)}\tau(z_{i2})\right)}{\sum_{i=1}^N \left(a_{22}^{(1)}\tau(z_{i1}) + a_{22}^{(2)}\tau(z_{i2})\right)} \\
&+ \frac{\sum_{i=1}^N \left((X_{i1} - \mu_{10}^{(m)})a_{12}^{(1)}\tau(z_{i1}) + (X_{i1} - \mu_{11}^{(m)})a_{12}^{(2)}\tau(z_{i2})\right)}{\sum_{i=1}^N \left(a_{22}^{(1)}\tau(z_{i1}) + a_{22}^{(2)}\tau(z_{i2})\right)} \\
\mu_{11}^{(m+1)} =& \frac{\sum_{i=1}^N X_{i1}\left(a_{11}^{(2)}\tau(z_{i2}) + a_{11}^{(4)}\tau(z_{i4})\right)}{\sum_{i=1}^N \left(a_{11}^{(2)}\tau(z_{i2}) + a_{11}^{(4)}\tau(z_{i4})\right)} \\
&+ \frac{\sum_{i=1}^N \left((X_{i2} - \mu_{20}^{(m)})a_{12}^{(2)}\tau(z_{i2}) + (X_{i2} - \mu_{21}^{(m)})a_{12}^{(4)}\tau(z_{i4})\right)}{\sum_{i=1}^N \left(a_{11}^{(2)}\tau(z_{i2}) + a_{11}^{(4)}\tau(z_{i4})\right)} \\
\mu_{21}^{(m+1)} =& \frac{\sum_{i=1}^N X_{i2}\left(a_{22}^{(3)}\tau(z_{i3}) + a_{22}^{(4)}\tau(z_{i4})\right)}{\sum_{i=1}^N \left(a_{22}^{(3)}\tau(z_{i3}) + a_{22}^{(4)}\tau(z_{i4})\right)} \\
&+ \frac{\sum_{i=1}^N \left((X_{i1} - \mu_{10}^{(m)})a_{12}^{(3)}\tau(z_{i3}) + (X_{i1} - \mu_{11}^{(m)})a_{12}^{(4)}\tau(z_{i4})\right)}{\sum_{i=1}^N \left(a_{22}^{(3)}\tau(z_{i3}) + a_{22}^{(4)}\tau(z_{i4})\right)}.
\end{aligned}$$

1.4 Assign Initial Values and Identify the Components

We assign the initial values with the constraints we imposed as described in Section 2.1. When we use the EM algorithm, the parameters would converge at its local maximums, so the initial values are pretty important. To assign the initial values, we first fit a two-component normal mixture model (there are many other methods such as the K means or hierarchical clustering with clusters set to 2) on each data type separately (Benaglia et al., 2009), then we order the means based on its value and assign them as the initial values. This has greatly helped to preserve our prespecified labels of the components. However, we recognize that this may fail when the difference of the means between the null and alternative are small. In this situation, the readers need to reorganize the labels of the components based on the final converged mean parameters. We present a quick example here, let the global null component labeled as component 1 (data1-,data2-) and the other components ordered as the mean constraints indicated previously, i.e., component 2 (data1+,data2-), component 3 (data1-,data2+), component 4 (data1+,data2+). This is similar to three data types. This is a pretty straightforward task, as the means are set constrained, it is easy to identify the correct component label. For example, if the converged outcome gives us the mean vectors of each component as (0.56,1.13), (3.11,1.13), (0.56,0.26), (3.11,0.26). We could rearrange the orders based on the mean values and the constraints as comp1 (0.56,0.26), comp2 (3.11,0.26), comp3 (0.56,1.13), comp4 (3.11,1.13). Here, the null mean is 0.56 for data type 1 and 0.26 for data type 2; the alternative mean is 3.11 for data type 1 and 1.13 for data type 2.

2 Simulation Studies

2.1 Simulation Parameters Mimicking TCGA Bladder Cancer Real Data

The parameters used for multivariate normal mixture for simulation studies scenario 6 mimicking TCGA bladder cancer real data are shown here, $\hat{\pi}$=(0.268577053, 0.233897556, 0.189871018, 0.006866345, 0.256186213, 0.008889446, 0.010178071, 0.025534298), the mean vectors for the eight components are

$\boldsymbol{\mu_1} = (0.5012989, 0.3832367, 0.4550859)$; $\boldsymbol{\mu_2} = (3.6045370, 0.3832367, 0.4550859)$;

$\boldsymbol{\mu_3} = (0.5012989, 4.2595606, 0.4550859)$; $\boldsymbol{\mu_4} = (0.5012989, 0.3832367, 4.2136909)$;

$\boldsymbol{\mu_5} = (3.6045370, 4.2595606, 0.4550859)$; $\boldsymbol{\mu_6} = (3.6045370, 0.3832367, 4.2136909)$;

$\boldsymbol{\mu_7} = (0.5012989, 4.2595606, 4.2136909)$; $\boldsymbol{\mu_8} = (3.604537, 4.259561, 4.213691)$.

The covariance matrices for the eight components are

$$\boldsymbol{\Sigma_1} = \begin{pmatrix} 1.26 & 0.01 & 0.05 \\ 0.01 & 1.04 & 0.02 \\ 0.05 & 0.02 & 1.21 \end{pmatrix}; \boldsymbol{\Sigma_2} = \begin{pmatrix} 1.50 & -0.01 & -0.02 \\ -0.01 & 1.02 & -0.04 \\ -0.02 & -0.04 & 1.14 \end{pmatrix}; \boldsymbol{\Sigma_3} = \begin{pmatrix} 1.21 & 0.09 & 0.02 \\ 0.09 & 2.52 & -0.02 \\ 0.02 & -0.02 & 1.22 \end{pmatrix};$$

$$\boldsymbol{\Sigma_4} = \begin{pmatrix} 0.90 & 0.01 & 0.06 \\ 0.01 & 1.01 & 0.05 \\ 0.06 & 0.05 & 1.12 \end{pmatrix}; \boldsymbol{\Sigma_5} = \begin{pmatrix} 1.84 & 0.22 & -0.09 \\ 0.22 & 3.58 & -0.01 \\ -0.09 & -0.01 & 1.21 \end{pmatrix}; \boldsymbol{\Sigma_6} = \begin{pmatrix} 1.92 & -0.04 & 0.16 \\ -0.04 & 1.05 & -0.16 \\ 0.16 & -0.16 & 1.23 \end{pmatrix};$$

$$\boldsymbol{\Sigma_7} = \begin{pmatrix} 1.01 & 0.11 & 0.13 \\ 0.11 & 2.80 & 0.36 \\ 0.13 & 0.36 & 1.24 \end{pmatrix}; \boldsymbol{\Sigma_8} = \begin{pmatrix} 1.63 & 0.29 & 0.08 \\ 0.29 & 4.02 & 0.09 \\ 0.08 & 0.09 & 1.39 \end{pmatrix}.$$

2.2 Model Calibration Estimation

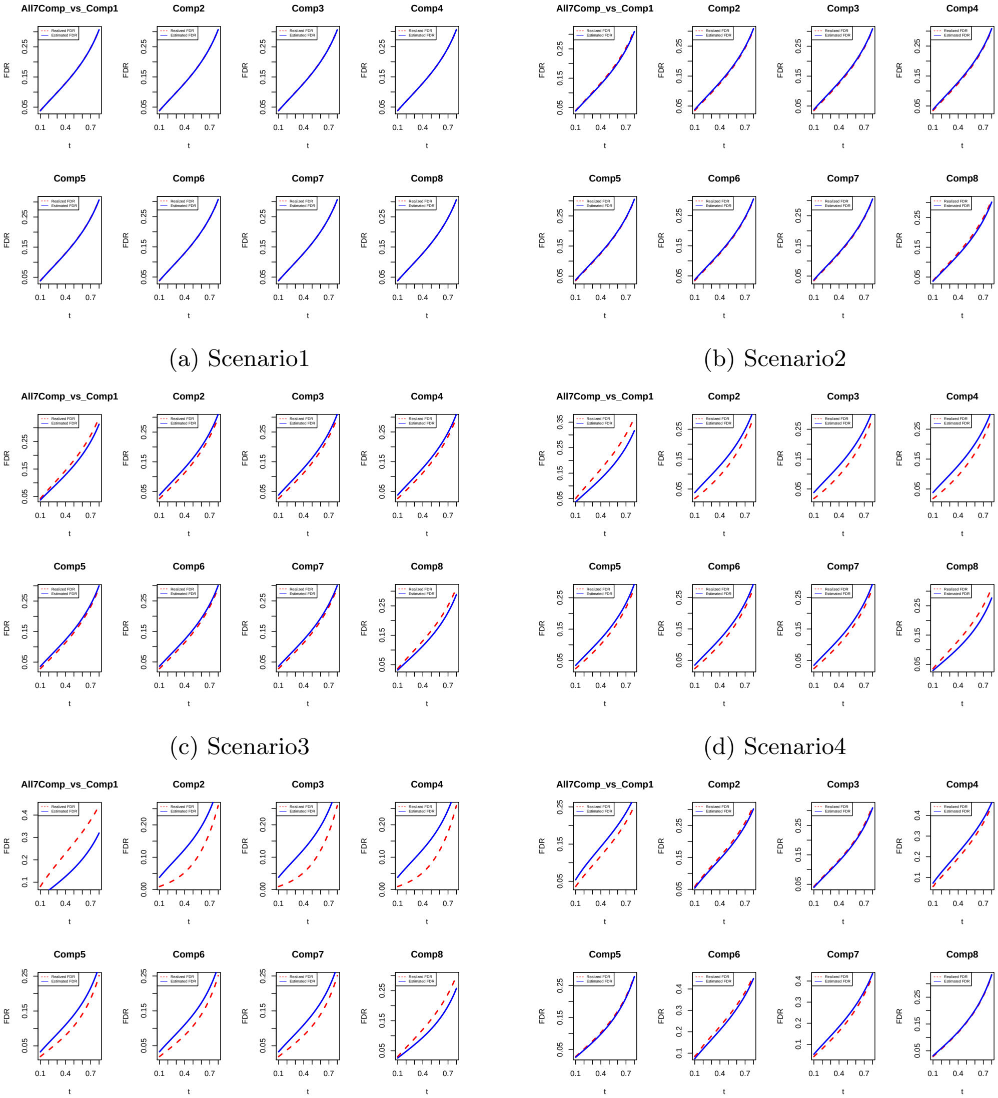

(a) Scenario1

(b) Scenario2

(c) Scenario3

(d) Scenario4

(e) Scenario5

(f) Scenario6

Figure 1: Model calibration of IMIX-Ind for 1000 simulation results.

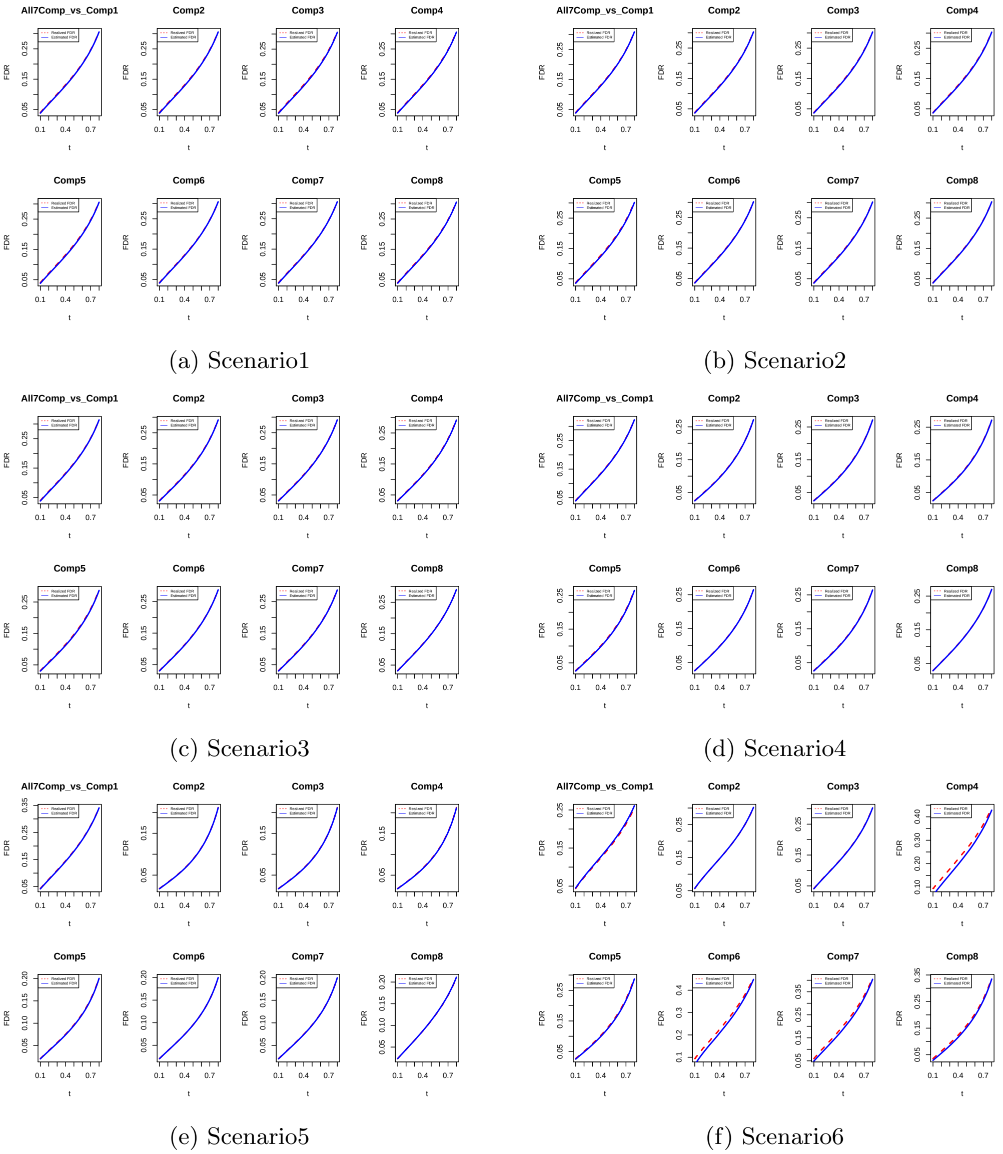

(a) Scenario1

(b) Scenario2

(c) Scenario3

(d) Scenario4

(e) Scenario5

(f) Scenario6

Figure 2: Model calibration of IMIX-Cor for 1000 simulation results.

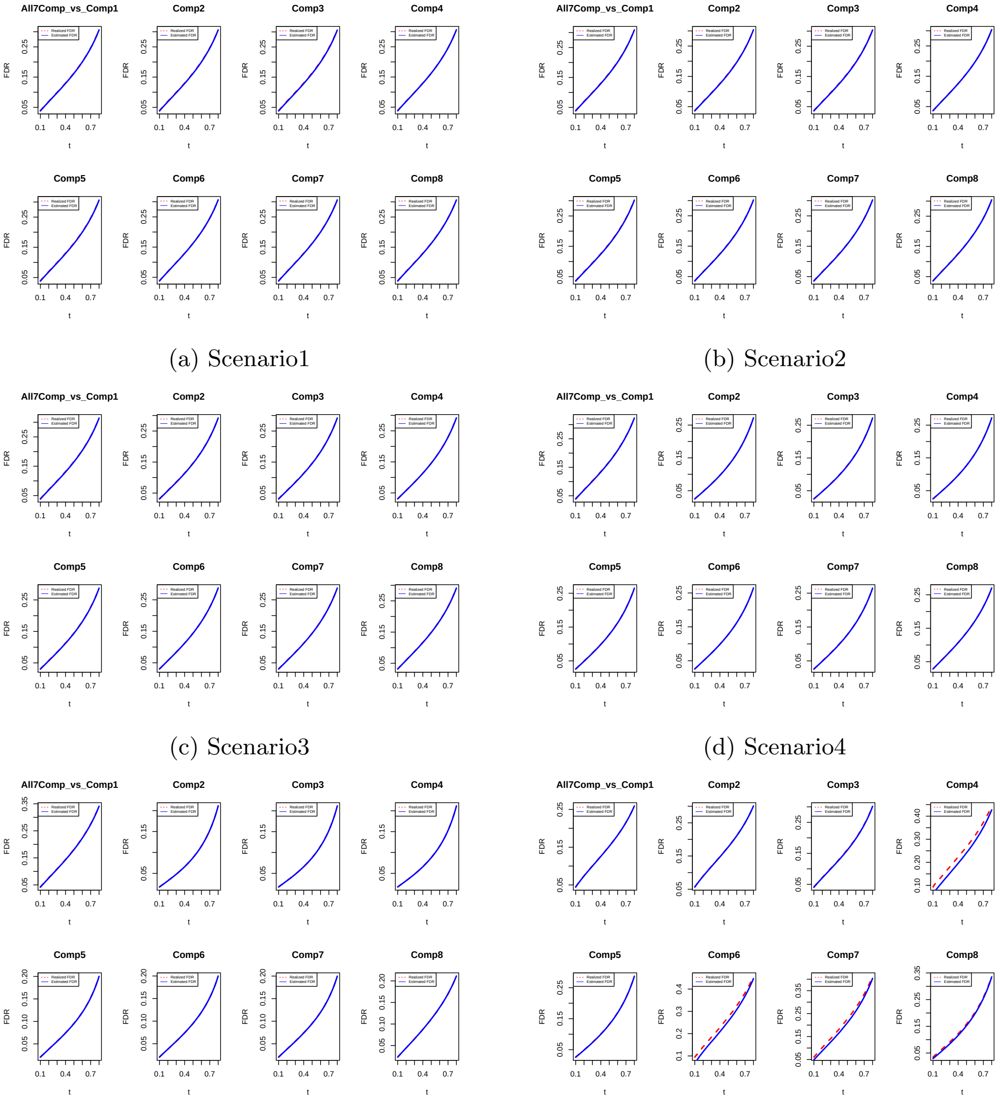

(a) Scenario1

(b) Scenario2

(c) Scenario3

(d) Scenario4

(e) Scenario5

(f) Scenario6

Figure 3: Model calibration of IMIX-Cor-Restrict for 1000 simulation results.

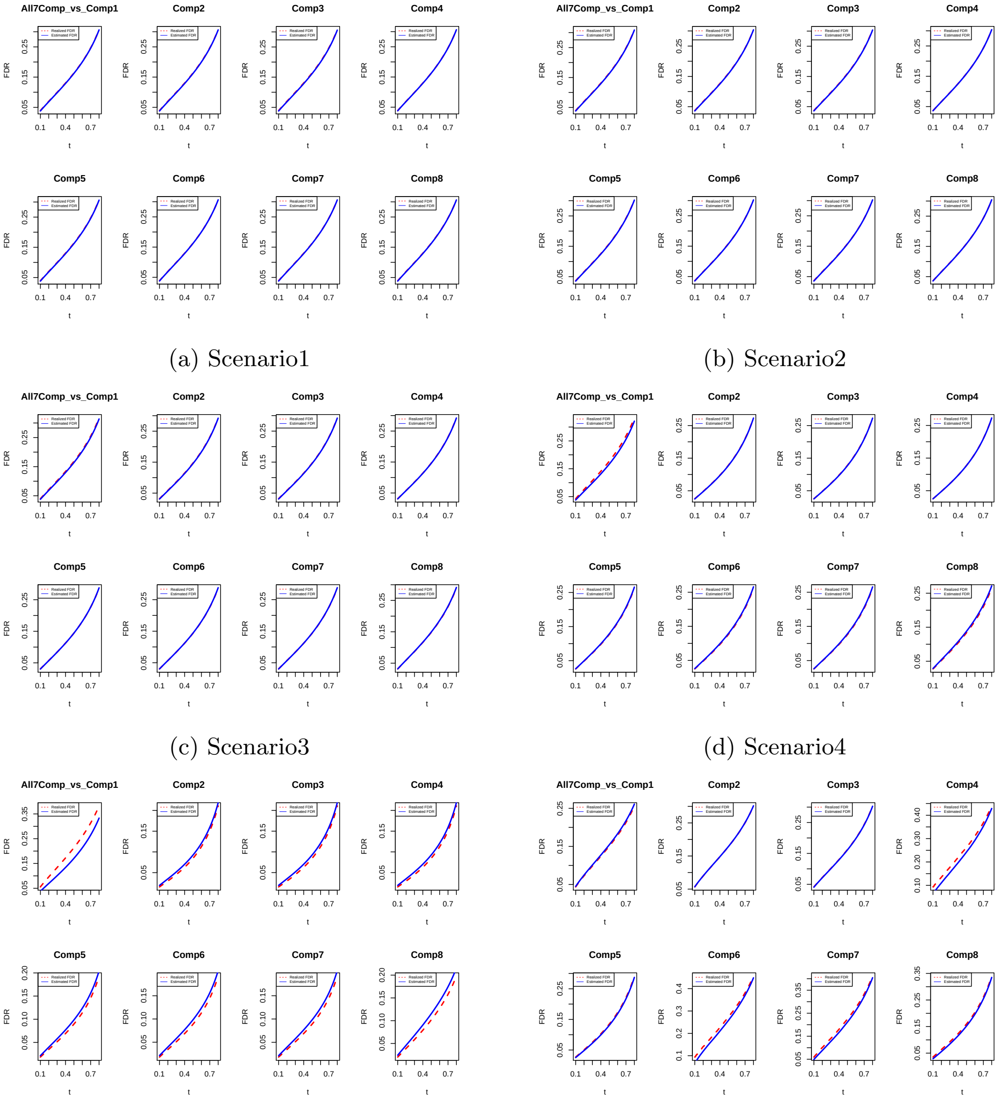

(a) Scenario1

(b) Scenario2

(c) Scenario3

(d) Scenario4

(e) Scenario5

(f) Scenario6

Figure 4: Model calibration of IMIX-Cor-Twostep for 1000 simulation results.

2.3 Model Selection

Number of Components	**Balanced**	**Unbalanced**
7 Components	(0.25,0.125,0.125,0.125,0.125,0.125,0.125)	(0.304,0.095,0.290,0.017,0.269,0.004,0.021)
8 Components	(0.125,0.125,0.125,0.125,0.125,0.125,0.125,0.125)	(0.300,0.095,0.290,0.017,0.269,0.004,0.021,0.004)

Table 1: Mixing proportions in simulation study setup 2. For each mixing proportion and number of components combination, we generated four scenarios with the mean and covariance parameters equal to the simulated parameters in simulation study 1 Scenarios 2-5. In total there are 16 simulation scenarios.

Let x_i be the group label, here we let it be from 1 to 8, $x_i = 1, \cdots, 8$. a is the slope, b is the intercept. Let

$$a \sum_{i=1}^{8} x_i + b = 1$$

Now we consider to solve this equation

$$\begin{cases} 36a + 8b = 1 \\ 8a + b = c \end{cases} \tag{1}$$

Here, we let $c = 0.005, 0.01, 0.05, 0.1$. Solve the equation and get the proportions for each component for the 4 scenarios, the proportion of component i would be $ax_i + b$.

	Proportion
c=0.1	(0.150,0.143,0.136,0.129,0.121,0.114,0.107,0.100)
c=0.05	(0.200,0.179,0.157,0.136,0.114,0.093,0.071,0.05)
c=0.01	(0.240,0.207,0.174,0.141,0.109,0.076,0.043,0.010)
c=0.005	(0.245,0.211,0.176,0.142,0.108,0.074,0.039,0.005)

Table 2: Mixing proportions in simulation study setup 3.

	Proportion
c=0.1	(0.129,0.129,0.129,0.129,0.128,0.128,0.128,0.100)
c=0.05	(0.136,0.136,0.136,0.136,0.136,0.135,0.135,0.05)
c=0.01	(0.144,0.141,0.141,0.141,0.141,0.141,0.141,0.010)
c=0.005	(0.143,0.142,0.142,0.142,0.142,0.142,0.142,0.005)

Table 3: Mixing proportions in simulation study setup 4, one group unbalance.

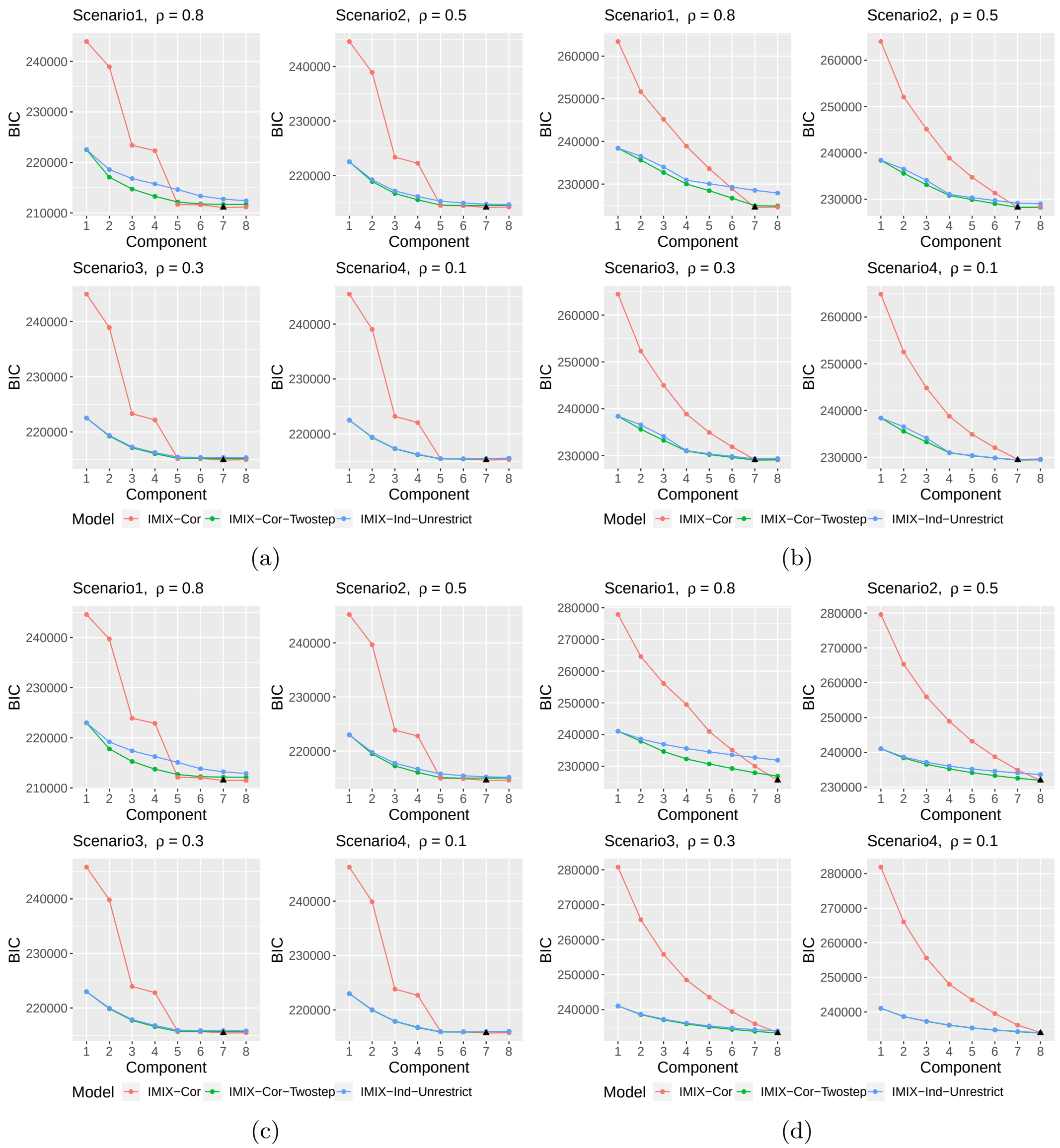

(a) (b)

(c) (d)

Figure 5: Simulation study on selecting the number of mixture components using BIC. (a) Unbalanced setting, 7-component mixture model. (b) Balanced setting, 7-component mixture model. (c) Unbalanced setting, 8-component mixture model. (d) Balanced setting, 8-component mixture model. Black triangle represents the model BIC selects. ρ is the correlation between data types.

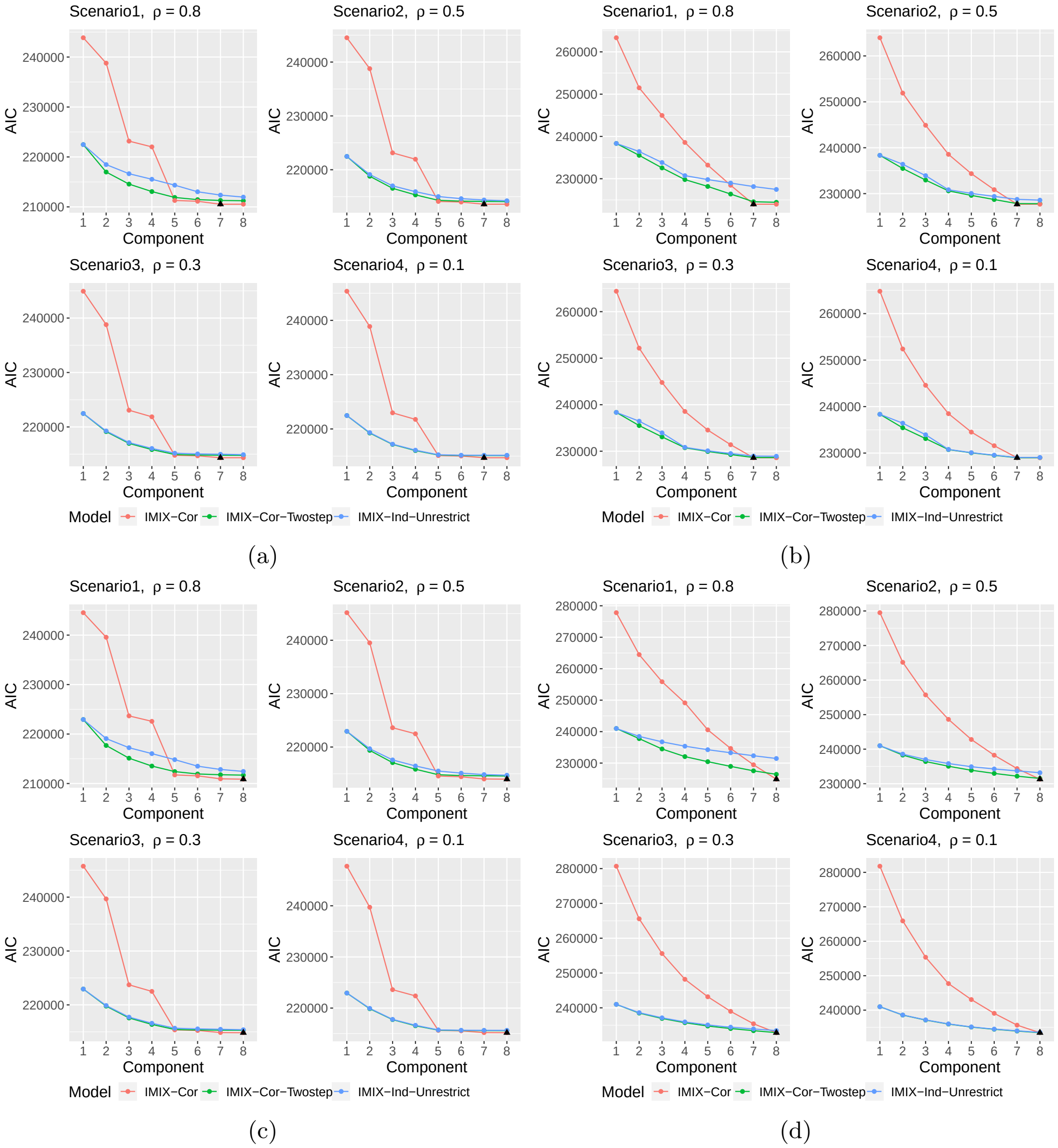

Figure 6: Simulation study on selecting the number of mixture components using AIC. (a)Unbalanced setting, 7-component mixture model. (b)Balanced setting, 7-component mixture model. (c)Unbalanced setting, 8-component mixture model. (d)Balanced setting, 8-component mixture model. Black triangle represents the model AIC selects. ρ is the correlation between data types.

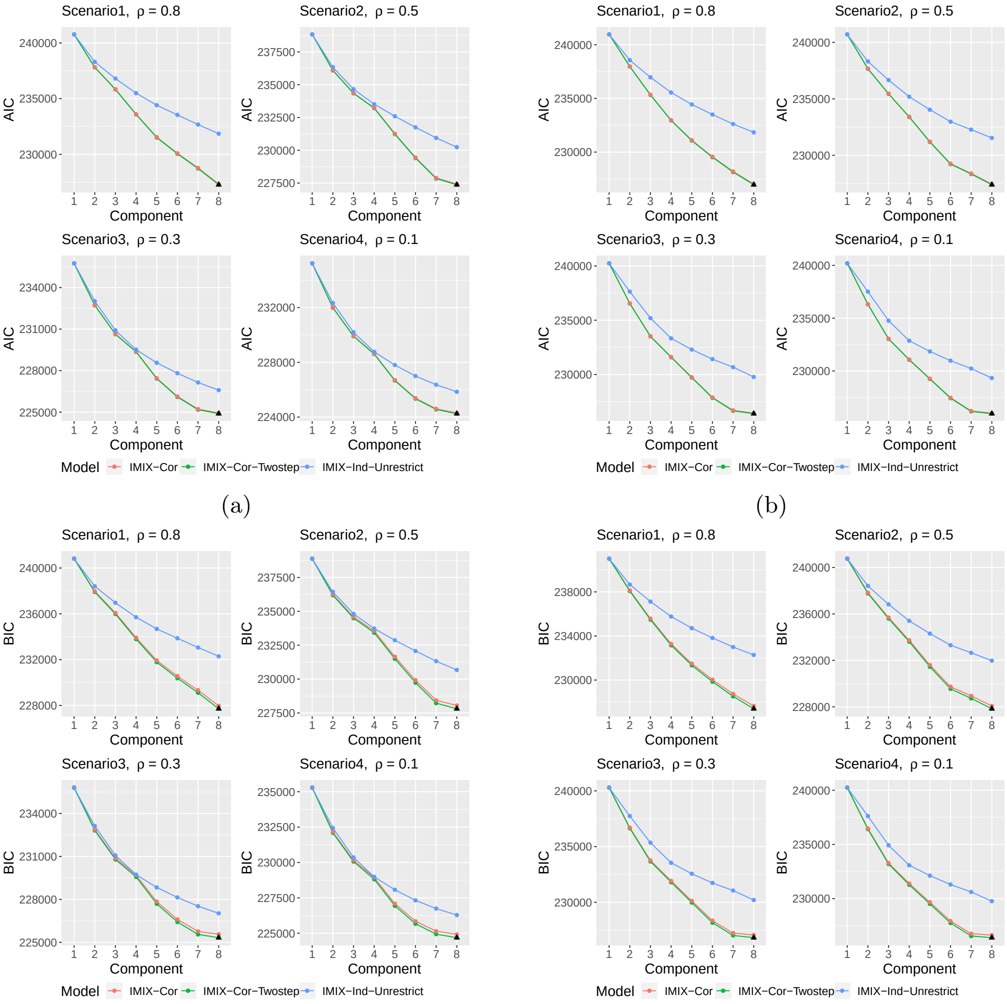

(a) (b)

(c) (d)

Figure 7: Model selection of AIC and BIC when the mixing proportions are unbalanced. AIC: (a) simulation set up 3. (b) simulation set up 4. BIC: (c) simulation set up 3. (d) simulation set up 4. Black triangle represents the model AIC/BIC selects. ρ is the correlation between data types.

2.4 Computational Time of IMIX

Computation time (in seconds)	Mean	SD
IMIX-Ind	4.501	0.879
IMIX-Cor	970.901	167.922
IMIX-Cor-Restrict	417.531	57.425
IMIX-Cor-Twostep	217.379	25.787

Table 4: Computational time needed (mean and standard deviation (SD) with 20 000 genes of $H = 3$ data types) for IMIX models under comparison in the simulation study 1 (Figure 1; Scenario 3 with data correlation of 0.3).

Number of iteration	Mean	SD
IMIX-Ind	67	8.652
IMIX-Cor	161	24.606
IMIX-Cor-Restrict	71	7.597
IMIX-Cor-Twostep	42	3.497

Table 5: Number of iterations needed (mean and standard deviation (SD) with 20 000 genes of $H = 3$ data types) for IMIX models under comparison in the simulation study 1 (Figure 1; Scenario 3 with data correlation of 0.3).

3 Real Data Applications to The Cancer Genome Atlas (TCGA)

3.1 Data Preprocessing and Quality Control

For bladder cancer in the TCGA, copy number variation (CNV) and methylation data were retrieved from TCGA2STAT (Wan et al., 2016), RNAseq data was retrieved from Broad Institute Genome Data Analysis Centers TCGA (http://gdac.broadinstitute.org/), and preprocessed and log-transformed previously as described in Guo et al. (2019). All three datasets were with reference genome build hg19. CNV was array-based level-3 gene-level data. Methylation data were measured on the Illumina Infinium HumanMethylation450 (450K)

BeadChip array at over 480,000 sites. The CpG sites with missing values in more than 10% of the total samples were filtered out. We excluded all the probes on the sex chromosomes, the probes of target polymorphic CpGs that overlaps with known SNPs (Fortin et al., 2017), and the probes that are cross-reactive (Chen et al., 2013). The methylation data were normalized using the Beta-Mixture Quantile (BMIQ) Normalization function from R package "wateRmelon" (Ruth, 2013). For downstream individual-level analysis, there were 373 DNA methylation samples, 391 RNA-Seq samples, and 387 CNV samples with $N = 15\,672$ genes.

Individual level test was conducted with respect to the binary molecular subtypes using logistic regression adjusting for the clinical covariates, including age, sex, race, smoking status, and pathological stage. The same procedure was conducted for RNAseq and CNV data. For probe level methylation data, we conducted the set-based test within each gene, the sequence kernel association test (SKAT) (Wu et al., 2011). The summary statistics P-value was collected for the three data types, and then transformed to z-scores for IMIX analysis.

For pancreatic cancer in the TCGA, we preprocessed the CNV data with the same quality control procedures as the bladder cancer dataset. The level-3 RSEM RNAseq data were retrieved from TCGA2STAT (Wan et al., 2016) and log-transformed. The same preprocessing procedure on the samples was performed. Individual-level test was conducted for the time-to-event outcome using the Cox proportional hazards model to each of the $15\,472$ genes respectively on 157 RNA-Seq samples and 161 CNV samples adjusting for age, gender, and smoking status. The summary statistics P-values were collected for the two data types, and then transformed to z-scores for IMIX analysis.

The molecular subtypes of bladder cancer patients in the TCGA were retrieved from previous work (Guo et al., 2019).

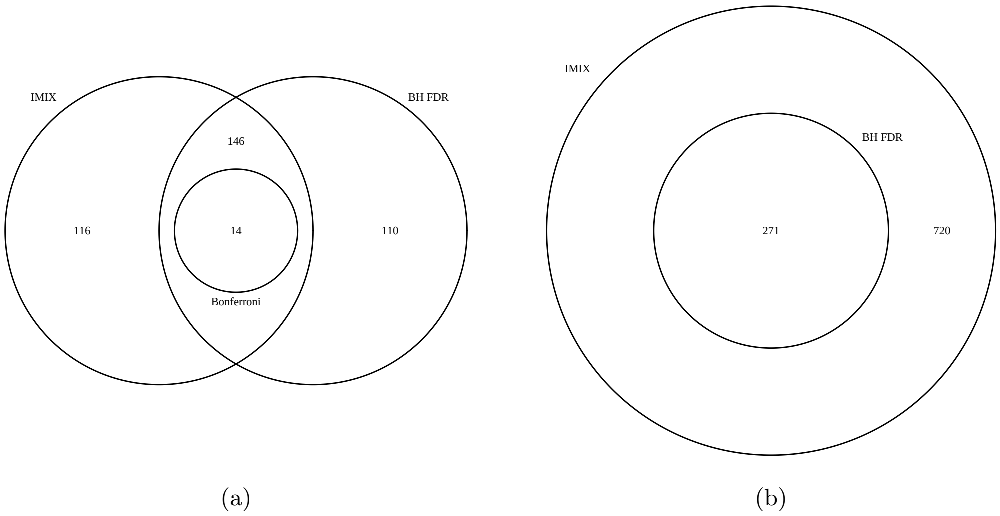

(a)

(b)

Figure 8: Comparisons between the number of significant genes in the TCGA datasets detected by the IMIX framework, Benjamini-Hochberg FDR (BH-FDR), and Bonferroni correction. (a) Number of genes detected by the IMIX framework, BH-FDR, and Bonferroni correction that are associated with the molecular subtypes of muscle-invasive bladder cancer through DNA methylation, gene expression, and CNV, with adaptive FDR control at $\alpha = 0.2$, estimated $\widehat{\text{mFDR}}_8 = 0.1995$. (b) Number of genes detected by IMIX and BH-FDR that are associated with the survival status of pancreatic cancer patients through gene expression and CNV, with adaptive FDR control at $\alpha = 0.2$, estimated $\widehat{\text{mFDR}}_4 = 0.2$.

3.2 The Directed Acyclic Graphs (DAGs) of 61 Significant Genes in Component 8

We estimated the causal relationships between DNA methylation, gene expression, and CNV of the 61 genes in component 8 by applying Bayesian networks (Scutari, 2017) with the target nominal type I error rate at 0.01. The directed acyclic graphs (DAGs) based on conditional independence tests with a restriction of causal direction from CNV to E showed six different patterns of causal structures for our data. In particular, seven genes had a full model with connections of CNV→E, E−M, M−CNV (Fig S8(1)); five genes showed causal effect of both CNV and DNA methylation on gene expression, while CNV and DNA methylation were marginally independent (Fig S8(2)); 17 genes had a reactive model as CNV→E→M (Fig S8(3)), which had also been reported by previous research (Sun et al., 2018). Seventeen genes showed that DNA methylation and gene expression were conditionally independent given CNV as M−CNV→E (Fig S8(4)) with the causal direction between CNV and DNA methylation indistinct from the statistical test. One gene showed conditional independence between CNV and gene expression given DNA methylation (Fig S8(5)); however, the direction of the DAG was not available due to the Markov equivalence, i.e., all three scenarios (CNV → M→E; E→M→CNV; CNV←M→E) led to conditional independence. This model was likely to be a true causal model as CNV→M→E. Four genes showed a dependence structure between gene expression and CNV given DNA methylation (Fig S8(6)). The rest of the ten genes showed no triangular association pattern.

3.3 A Sensitivity Analysis of Overlapped and Non-Overlapped Samples

The patients can be partially overlapped or completely different across the data types as the method only involves summary statistics for analysis. We have performed a sensitivity analysis in the TCGA bladder cancer data to show this feature. As proof of concept, we used only CNV and RNAseq data. We first matched the samples across the two data types (n=371) and randomly split them into two halves. Analysis 1 was based on the same set of samples in the two data types. We used the same first half (n=185) of the samples across the two data types. Analysis 2 was based on two different sets of samples without overlap in the two data types. We used the first half of samples (n=185) for CNV data and the second half of samples (n=186) for RNAseq data. We compared the results from the two analyses based on the Benjamini-Hochberg FDR control at 0.05 for each data type separately and IMIX-Cor-Twostep with across-data-type FDR at 0.2, as shown in the table below.

	BH-FDR (not consider correlation)				**IMIX-Cor-Twostep**			
Analysis 2 Analysis 1	1 (GE-,CNV-)	2 (GE+,CNV-)	3 (GE-,CNV+)	4 (GE+,CNV+)	1 (GE-,CNV-)	2 (GE+,CNV-)	3 (GE-,CNV+)	4 (GE+,CNV+)
1 (GE-,CNV-)	7475	1738	120	53	8512	2352	16	51
2 (GE+,CNV-)	1461	4660	32	97	942	4164	0	0
3 (GE-,CNV+)	86	18	224	72	25	0	81	23
4 (GE+,CNV+)	33	69	67	253	27	0	18	247

Table 6: Results of the sensitivity analysis comparing same samples (analysis 1) and different samples (analysis 2) in the TCGA bladder cancer data using only gene expression and CNV data.

We conclude that despite the expected difference between the actual individual samples that may result in the difference as illustrated in the BH-FDR method, IMIX performed well in returning a robust result. Specifically, comparing the results of analysis 1 and analysis 2, where one used the same sample set and the other used complete different samples, both returned 8512 genes in component 1 (GE-,CNV-), 4164 genes in component 2 (GE+,CNV-), 81 genes in component 3 (GE-,CNV+), and 247 genes in component 4 (GE+,CNV+).

Analysis: bladder_fdr001_adaptive - 2020-02-20 12:21 PM

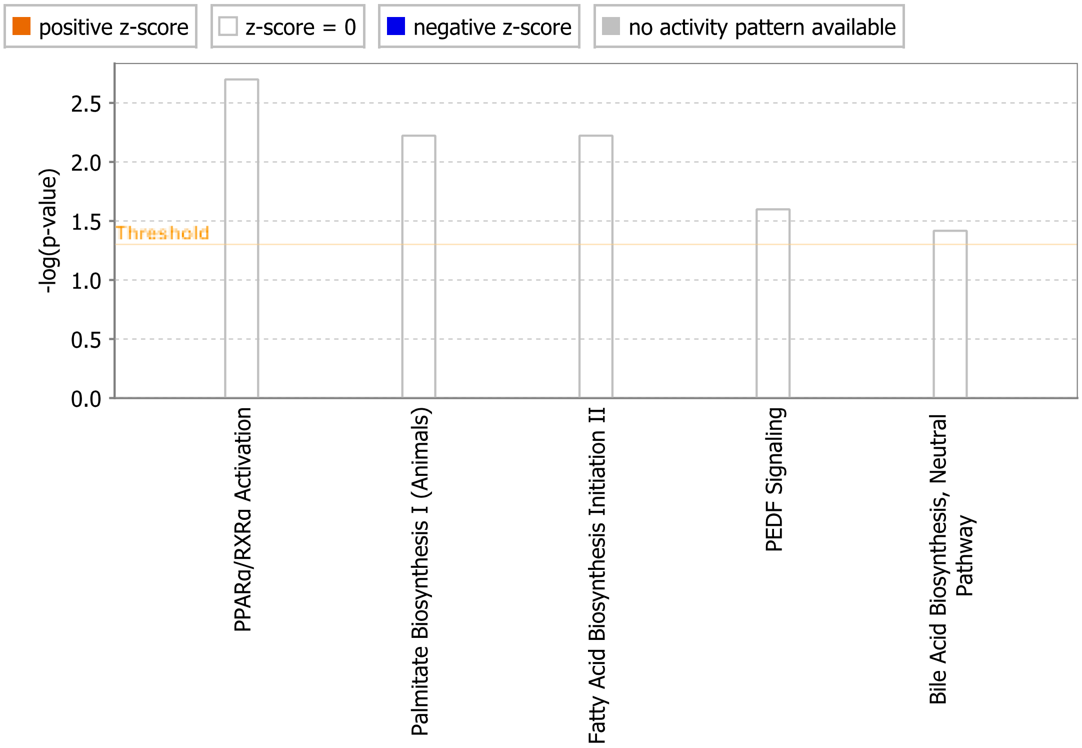

Figure 9: The canonical pathways identified by the Ingenuity Pathway Analysis (IPA) on the 61 significant genes in component 8 with adaptive FDR controlled at $\alpha = 0.01$ of bladder cancer subtypes in the TCGA.

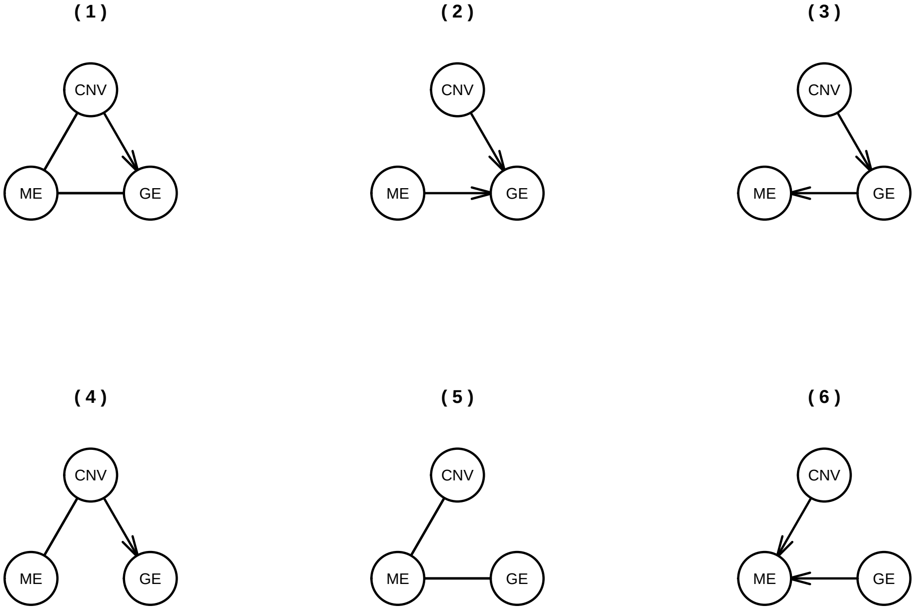

Figure 10: The Directed acyclic graphs (DAGs) based on Bayesian network with a restriction of causal direction from CNV to gene expression for the genes in component 8 of TCGA bladder cancer with across-data-type FDR controlled at $\alpha = 0.01$.

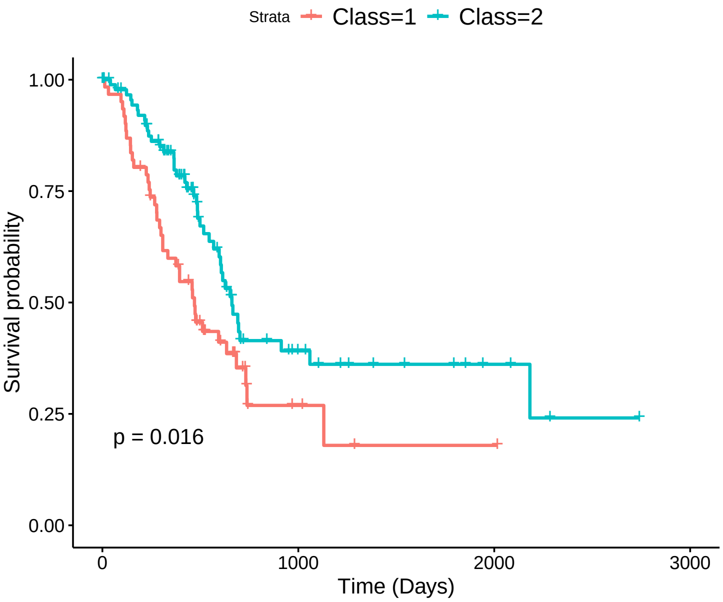

Figure 11: Results of IMIX analysis for pancreatic cancer prognosis in the TCGA. Kaplan-Meier curves for pancreatic cancer patient survival in the TCGA. Samples were clustered based on the 104 genes identified by IMIX, with adaptive FDR control at $\alpha = 0.05$, estimated marginal FDR $(\widehat{\text{mFDR}}_4) = 0.0498$.

References

Benaglia, T., D. Chauveau, D. R. Hunter, and D. Young (2009). mixtools: An R package for analyzing finite mixture models. *Journal of Statistical Software 32*(6), 1–29.

Chen, Y.-a., M. Lemire, S. Choufani, D. T. Butcher, D. Grafodatskaya, B. W. Zanke, S. Gallinger, T. J. Hudson, and R. Weksberg (2013). Discovery of cross-reactive probes and polymorphic cpgs in the illumina infinium humanmethylation450 microarray. *Epigenetics 8*(2), 203–209.

Fortin, J.-P., T. J. Triche Jr, and K. D. Hansen (2017). Preprocessing, normalization and integration of the illumina humanmethylationepic array with minfi. *Bioinformatics 33*(4), 558–560.

Guo, C. C., T. Majewski, L. Zhang, H. Yao, J. Bondaruk, Y. Wang, S. Zhang, Z. Wang, J. G. Lee, S. Lee, et al. (2019). Dysregulation of emt drives the progression to clinically aggressive sarcomatoid bladder cancer. *Cell reports 27*(6), 1781–1793.

Ruth, P. (2013). Y wong chloe c, volta manuela, lunnon katie, mill jonathan, schalkwyk leonard c. a data-driven approach to preprocessing illumina 450k methylation array data. *BMC Genomics 14*(1), 293.

Scutari, M. (2017). Bayesian network constraint-based structure learning algorithms: Parallel and optimized implementations in the bnlearn r package. *Journal of Statistical Software, Articles 77*(2), 1–20.

Sun, W., P. Bunn, C. Jin, P. Little, V. Zhabotynsky, C. M. Perou, D. N. Hayes, M. Chen, and D.-Y. Lin (2018). The association between copy number aberration, dna methylation and gene expression in tumor samples. *Nucleic acids research 46*(6), 3009–3018.

Wan, Y.-W., G. I. Allen, and Z. Liu (2016). Tcga2stat: simple tcga data access for integrated statistical analysis in r. *Bioinformatics 32*(6), 952–954.

Wu, M. C., S. Lee, T. Cai, Y. Li, M. Boehnke, and X. Lin (2011). Rare-variant association testing for sequencing data with the sequence kernel association test. *The American Journal of Human Genetics 89*(1), 82–93.